

## Upper limits for the $^{27}\text{Al} + ^{16}\text{O}$ and $^{93}\text{Nb} + ^{16}\text{O}$ radiative-capture cross sections

D. Branford\* and S. G. Steadman

Laboratory for Nuclear Science, Massachusetts Institute of Technology, Cambridge, Massachusetts 02139

(Received 14 August 1978)

Thick targets of high purity aluminium and niobium were bombarded with  $^{16}\text{O}$  ions in the energy range 50–65 MeV. The yields of reaction products were obtained off-line using a Ge(Li) detector to observe residual  $\gamma$  activities. Ungated  $\gamma$  spectra and  $\gamma$  spectra in coincidence with pairs of 511 keV annihilation quanta, observed in an array of four  $7.5 \times 7.5$  cm NaI(Tl) detectors, were recorded. Upper limits of  $0.2\mu\text{b}$  and  $0.1\mu\text{b}$  were obtained for the  $^{27}\text{Al}(^{16}\text{O}, \gamma)^{43}\text{Sc}$  and  $^{93}\text{Nb}(^{16}\text{O}, \gamma)^{109}\text{In}$  radiative capture cross sections, respectively. These limits are compared to previously reported data and to the results of statistical model calculations. It is concluded that some previously reported total heavy-ion radiative capture results may be in error and tentative explanations for this are offered.

NUCLEAR REACTIONS  $^{27}\text{Al} + ^{16}\text{O}$ ,  $^{93}\text{Nb} + ^{16}\text{O}$ ,  $E = 50\text{--}65$  MeV; measured upper limits for yields of activation products  $^{43}\text{Sc}$  and  $^{109}\text{In}$ ; calculated cross sections. Natural targets, Ge(Li) and NaI(Tl) detectors.

### I. INTRODUCTION

Heavy-ion radiative capture (referred to hereafter as HIC) has been investigated previously for a range of target and projectile nuclei. In the lighter nuclei, one of the methods used is to detect the prompt high-energy  $\gamma$ -ray decay leading to low-lying bound states in the compound nucleus. Measurements of this type in which capture  $\gamma$  rays were observed have been made for the reactions  $^6\text{Li}$ ,  $^7\text{Li}$ ,  $^{12}\text{C}$ ,  $^{16}\text{O}(^{16}\text{O}, \gamma)$  and  $^{11}\text{B}$ ,  $^{12}\text{C}(^{12}\text{C}, \gamma)$  by Feldman and Heikinen<sup>1</sup> and for  $^{12}\text{C}(^{12}\text{C}, \gamma)$  by Sandorfi and Nathan.<sup>2</sup> The inverse HIC reactions  $^{24}\text{Mg}(\gamma, ^{12}\text{C})^{12}\text{C}$  has also been observed.<sup>3</sup> Typical measured cross sections are  $\sigma \sim 20$  nb  $\text{sr}^{-1}$  with the exception of those for the  $^7\text{Li}(^{16}\text{O}, \gamma)^{23}\text{Na}$  and  $^{12}\text{C}(^{12}\text{C}, \gamma)^{24}\text{Mg}$  reactions which exhibit resonancelike peaks that exceed  $50$  nb  $\text{sr}^{-1}$ .

A sensitive method for determining total HIC cross sections is to bombard a thick target with a heavy-ion beam which has been chosen so that the compound nucleus is an easily identifiable radioactive isotope. The HIC yields can then be obtained from an off-line activation analysis of the target and cross sections determined from these yields using known or calculated stopping power data. The first measurements of this type, made by Coleman *et al.*<sup>4</sup> for the  $^{27}\text{Al}(^{16}\text{O}, \gamma)^{43}\text{Sc}$  and  $^{31}\text{P}(^{16}\text{O}, \gamma)^{47}\text{V}$  reactions at center-of-mass bombarding energies just above the Coulomb barrier, gave upper limits of  $0.2\mu\text{b}$  and  $18\mu\text{b}$ , respectively, for the cross sections. More recently, Zeller *et al.*<sup>5</sup> obtained results of  $\sigma \sim 10\mu\text{b}$  for the  $^{30}\text{Si}(^{14}\text{N}, \gamma)^{44}\text{Sc}$  reaction over the bombarding energy range 40–60 MeV. Also, measurements of a similar nature by Imazato<sup>6</sup> for the  $^{16}\text{O}(^{32}\text{S}, \gamma)^{48}\text{Cr}$  and

$^{40}\text{Ca}(^{12}\text{C}, \gamma)^{52}\text{Fe}$  reactions gave radiative capture widths that correspond to a HIC cross section of  $\sigma \sim 10\mu\text{b}$ .

A significant feature of the  $^{30}\text{Si}(^{14}\text{N}, \gamma)^{44}\text{Sc}$  result is that the cross section rises with increasing bombarding energy over the range studied. This is explained by Zeller *et al.* using a model proposed for heavier systems by Grover and Gilat.<sup>7</sup> In this model, it is assumed that when the heavy ions coalesce to form a compound nucleus, there is a small but significant probability for populating states with excitation energies  $E_x$  and spins  $J$  near to the yrast line. It is then further assumed that these states decay by a cascade through other yrastlike states to the ground state. Zeller *et al.* also show that calculations made using this model agree with the measured cross sections if reasonable values for the moment of inertia of the compound systems are assumed.

An alternative method was used by Imazato in considering the  $^{40}\text{Ca}(^{12}\text{C}, \gamma)^{52}\text{Fe}$  data. He assumed that HIC in "light" heavy-ion systems is due primarily to statistical high energy  $\gamma$  decays from the highly excited compound nucleus to low-lying states for which particle decay is unlikely or energetically impossible. Calculations made by Imazato using this model agree both with the results for the reaction  $^{40}\text{Ca}(^{12}\text{C}, \gamma)^{52}\text{Fe}$  leading to the  $^{52}\text{Fe}$  ground state and to the  $J^\pi = 12^+$ , 62s isomeric state at 6.83 MeV. Both measurements report relatively large cross sections for HIC. Yet, in the measurements of Imazato, a large correction for contamination was made.

We report here on a study of the  $^{27}\text{Al}(^{16}\text{O}, \gamma)^{43}\text{Sc}$  and  $^{93}\text{Nb}(^{16}\text{O}, \gamma)^{109}\text{In}$  reactions which were made to investigate the HIC process further and perform

a contamination-free measurement. Both sets of measurements were made by bombarding thick targets with  $^{16}\text{O}$  ions and using an off-line Ge(Li) detector to search for characteristic  $\gamma$  radiations from the appropriate compound nuclei. In Sec. II we discuss the experimental method, in Sec. III the results and in Sec. IV we show calculations which are consistent with the results and offer an explanation for the discrepancy with the previous measurements.

## II. EXPERIMENTAL METHOD

An ingot of 99.9999% pure Al was cut into 2 mm thick targets using a diamond saw. Immediately before each bombardment, a target was etched for a few minutes in a solution of 10 g NaOH dissolved in 50 cl of distilled water at 40°C. The chemical etching was stopped by briefly immersing the target in concentrated nitric acid and rinsing it with distilled water. The target was then dried in air and mounted on the inside surface of a removable plate which formed the "downstream" wall of a small target chamber.

This chamber was evacuated to a pressure of  $5 \times 10^{-4}$  p ( $3 \times 10^{-6}$  Torr) and a vapor trap near the target was filled with liquid  $\text{N}_2$ . The target was then bombarded for 4 h by a beam of approximately  $2 \mu\text{A}$   $6^+$  or  $7^+$   $^{16}\text{O}$  ions from the Brookhaven National Laboratory MP6 tandem Van de Graaff accelerator. The integrated beam current was monitored using the chamber as a Faraday cup. The emission of secondary electrons from the collimator in the direction of the target chamber was suppressed using a flat plate which had a 1 cm diameter aperture in it to let the beam pass through. This plate was maintained at a potential of 100 V negative. Bombardments on different targets were made at 50, 55, 60, and 65 MeV.

Approximately four hours after bombardment each target was sandwiched between 1 mm thick Al plates and placed on the front face of a  $50 \text{ cm}^3$  Ge(Li) detector. The purpose of the plates was to slow down and stop  $\beta^+$  particles so that their annihilation occurred near the target. Using a 4096 channel analyzer,  $\gamma$ -ray spectra were recorded for 1 h intervals either ungated or in coincidence with pairs of 511 keV  $\gamma$  pulses observed in diagonal detectors of an array consisting of four  $7.5 \text{ cm} \times 7.5 \text{ cm}$  NaI detectors placed symmetrically around the target, with their front faces 3.75 cm from the target and their axes of symmetry at right angles to the Ge(Li) detector axis of symmetry. The efficiency for detecting pairs of 511 keV  $\gamma$  pulses was measured at 2 h intervals using a  $^{24}\text{Na}$  source. The Ge(Li) detector full-energy-peak efficiency was determined after the experiment using a

standard set of calibrated  $\gamma$  sources.

The above experimental method was also used to study the  $^{93}\text{Nb} + ^{16}\text{O}$  system. In this case, the targets were 250  $\mu\text{m}$  thick foils of 99.995% pure Nb. No attempts were made to etch the surfaces. A run was also made in which a thick Si slice was bombarded with 60 MeV ions for 20 min. This provided a useful check of the system and gave an indication of the effects of any Si contamination of the targets.

## III. RESULTS

Selected regions of spectra obtained using the  $^{27}\text{Al} + ^{16}\text{O}$  reaction are shown in Figs. 1 and 2. All the  $\gamma$ -ray peaks present in the full spectra were identified as arising from the decays of either  $^{34}\text{Cl}$  ( $T_{1/2} = 32.0$  min) or  $^{24}\text{Na}$  ( $T_{1/2} = 15.03$  h). Figure 3 summarizes the  $\beta$  decay information for the compound nucleus  $^{43}\text{Sc}$ . It has a half life of 3.92 h and decays by a 22% branch to the 373 keV  $\gamma$ -decaying state in  $^{43}\text{Ca}$  (16%  $\beta^+$  emission and 6% electron capture). Evidence for the  $^{27}\text{Al}(^{16}\text{O}, \gamma)^{43}\text{Sc}$  HIC reaction would, therefore, be given by the observation of a 373 keV full-energy peak in either the ungated or coincidence spectrum. To determine whether or not a small but statistically significant 373 keV peak was present in our data, the appropriate regions of the spectra were summed. The number of background counts were determined from the number of counts in adjacent regions and subtracted. The remaining counts  $N$  were used to give values for the yields of  $^{43}\text{Sc}$  produced in the bombardment per  $^{16}\text{O}$  ion by means of the equation

$$Y = \frac{N T e M}{\epsilon B C \tau} [1 - \exp(-T/\tau)]^{-1} \times [\exp(-t_1/\tau) - \exp(-t_2/\tau)]^{-1}, \quad (1)$$

where  $Y$  is the yield per incident ion,  $T$  is the bombardment time,  $e$  is the proton charge,  $M$  is the charge state of incident ions,  $\epsilon$  is the full-energy-peak efficiency,  $B$  is the fraction of decays giving rise to the  $\gamma$  ray,  $C$  is the total charge deposited in target,  $\tau$  is the mean nuclear lifetime,  $t_1$  is the start of spectrum recording time from end of bombardment, and  $t_2$  is the end of spectrum recording time from end of bombardment. This expression was also used for the coincidence data in which case  $\epsilon$  is the full-energy-peak efficiency for observing the  $\gamma$  rays in coincidence with pairs of 511 keV annihilation quanta and  $B$  is the fraction of  $\beta^+$  decays giving rise to the  $\gamma$  ray.

Figure 4 shows  $^{43}\text{Sc}$  yield results obtained from spectra recorded at different times following the 65 MeV bombardment. The mean of these data

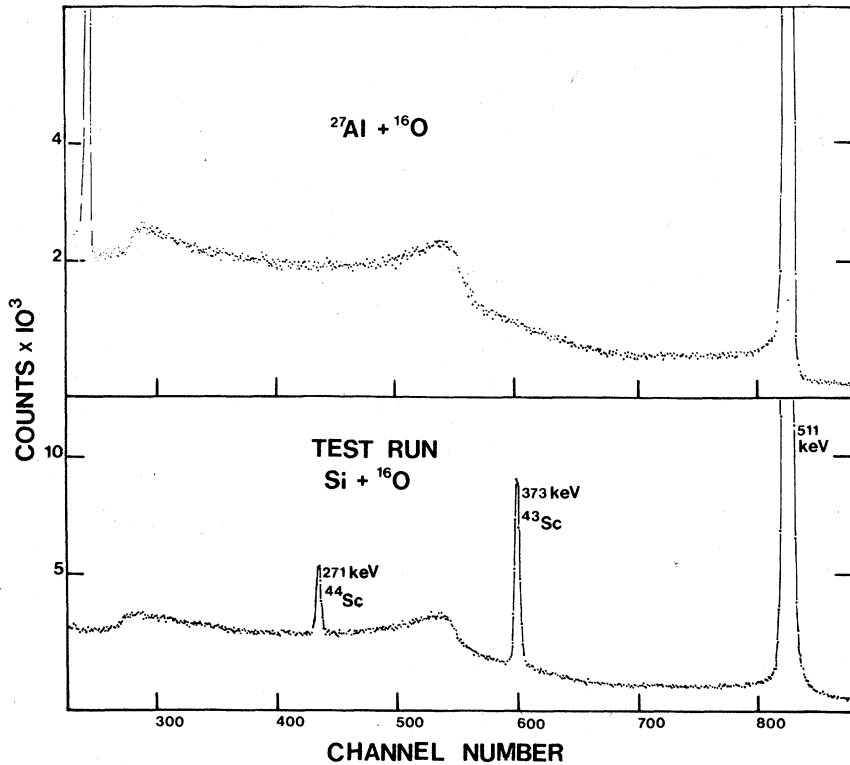


FIG. 1. *Upper part.* Portion of ungated spectrum recorded for 1 h following  $^{16}\text{O}$  bombardment of  $^{27}\text{Al}$  at 60 MeV. Start time  $t_1 = 6$  h 8 min from end of bombardment. *Lower part.* Portion of ungated spectrum recorded for 4.3 min following  $^{16}\text{O}$  bombardment of Si at 65 MeV. Start time  $t_1 = 1$  h from end of bombardment.

and the results obtained at 60 MeV gave no indication of  $^{43}\text{Sc}$  having been produced. By combining these means, an upper limit of  $Y < 4 \times 10^{-11}$  nuclei per incident ion at a confidence level of  $2\sigma$  was obtained.

The data at 50 and 55 MeV indicated that a significant number of  $^{43}\text{Sc}$  nuclei had been produced. However, the singles data also showed the presence of a 273 keV peak and the coincidence data contained an 1165 keV peak. These peaks indicate

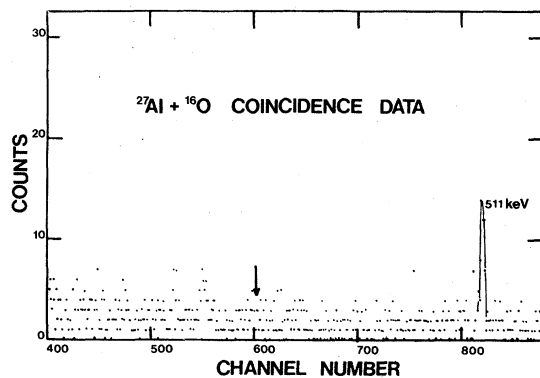


FIG. 2. Portion of gated spectrum recorded for 1 h following  $^{16}\text{O}$  bombardment of  $^{27}\text{Al}$  at 60 MeV. Start time  $t_1 = 5$  h 18 min from end of bombardment. The arrow marks the position expected for a 373 keV full-energy peak.

that  $^{44}\text{Sc}$  nuclei were produced (see Fig. 3), which in turn indicates that the targets were contaminated with material of mass  $A > 27$ . The most likely source of this contamination was traces of natural Si caused by the deposition of oil vapor on the target while in the vacuum. This possibility was investigated by considering the natural Si data. These showed that the ratio of the  $^{44}\text{Sc}$  to  $^{43}\text{Sc}$  yield was approximately equal to the ratio obtained for the Al bombardment targets at 50 and 55 MeV. Since slight differences in this ratio are expected between thick and thin target yields, it is concluded that the  $^{43}\text{Sc}$  activities observed using the Al targets were most probably due to reactions taking place on traces of Si. The Al

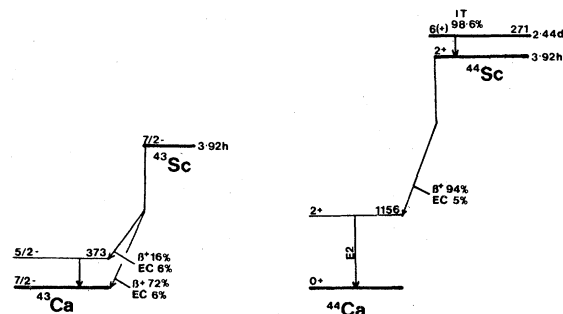


FIG. 3. Partial decay schemes for  $^{43}\text{Sc}$  and  $^{44}\text{Sc}$ .

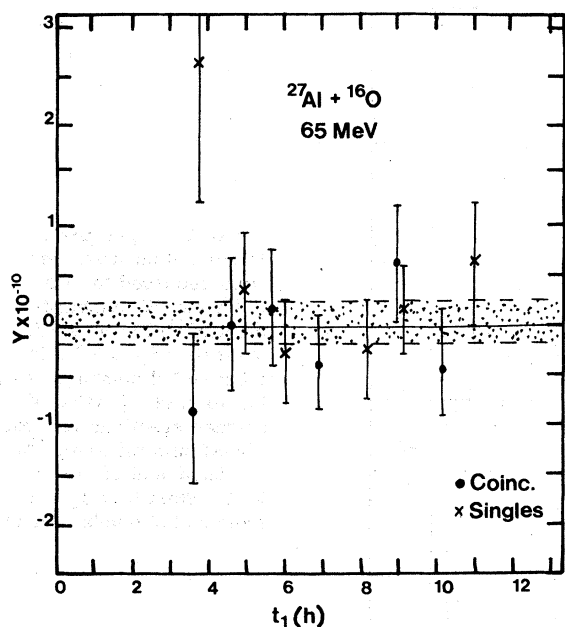


FIG. 4. Results of  $^{43}\text{Sc}$  yield measurements following  $^{16}\text{O}$  bombardment of  $^{27}\text{Al}$  at 65 MeV vs start time for recording spectrum from end of bombardment.

data at 50 and 55 MeV are, therefore, not considered further.

The cross section  $\sigma(E)$  is related to the yield by the equation

$$Y = N \int_0^{E_B} \frac{\sigma(E)}{[dE/dx(E)]} dE, \quad (2)$$

where  $N$  is the number of nuclei per kg of target material,  $E_B$  is the energy of beam in MeV, and  $dE/dx$  is the stopping power in  $\text{MeV kg m}^{-2}$ . From Eq. 2, it follows that an approximate expression for the average cross section  $\bar{\sigma}$  between  $E_B$  and the laboratory energy  $E_c$  corresponding to the Coulomb barrier (effective lower limit for the capture reaction) is

$$\bar{\sigma} \approx Y/N [R(E_B) - R(E_c)]^{-1}, \quad (3)$$

where  $R(E)$  is the range in  $\text{kg m}^{-2}$  for ions with energy  $E$ .

Equation 3 was used to obtain an upper limit for  $\bar{\sigma}$  from the result  $Y < 4 \times 10^{-11}$  nuclei per incident ion presented earlier. The energy  $E_c$  was calculated to be 28.8 MeV using a radius parameter of  $r_0 = 1.5$  fm. The ranges  $R(E_B)$  and  $R(E_c)$  were obtained from the calculated results of Northcliffe and Schilling.<sup>8</sup> This gave  $\bar{\sigma} < 0.2 \mu\text{b}$  ( $2\sigma$ ) for the  $^{27}\text{Al}(^{16}\text{O}, \gamma)^{43}\text{Sc}$  HIC average cross section in the bombarding energy range 28.8–62.5 MeV.

A selected region of a typical spectrum from the  $^{93}\text{Nb} + ^{16}\text{O}$  reaction is shown in Fig. 5. The full

spectrum contained many  $\gamma$  peaks from the decays of reaction products, such as  $^{103}\text{Ag}$  ( $T_{1/2} = 1.1$  h),  $^{104}\text{Ag}^*$  (33.5 m),  $^{104}\text{Cd}$  (57.7 m),  $^{105}\text{Cd}$  (55 m),  $^{109}\text{In}$  (32.4 m), etc. The compound nucleus for this system,  $^{109}\text{In}$ , has a half life of 4.2 h and gives rise to 203 keV  $\gamma$  rays. A search for the full-energy peak at this energy was made using only singles data since the low probability for  $\beta^+$  decay (7.9%) compared to the total decay to the 203 keV state in  $^{109}\text{Cd}$  (78.4%) gives rise to a relatively poor sensitivity for the coincidence method. The small 205 keV  $^{107}\text{In}$  peaks (see Fig. 5) were subtracted off. Proceeding in the same manner as that used for the  $^{27}\text{Al} + ^{16}\text{O}$  reaction, results of  $Y < 2 \times 10^{-12}$  nuclei per incident ion ( $2\sigma$ ) were obtained for  $^{109}\text{In}$  production at 50, 55, and 60 MeV. Using a calculated  $E_c = 52$  MeV, the 60 MeV data gives a result of  $\bar{\sigma} < 0.1 \mu\text{b}$  ( $2\sigma$ ) for the  $^{93}\text{Nb}(^{16}\text{O}, \gamma)^{109}\text{In}$  HIC average cross section over the bombarding energy range 52–60 MeV.

#### IV. DISCUSSION

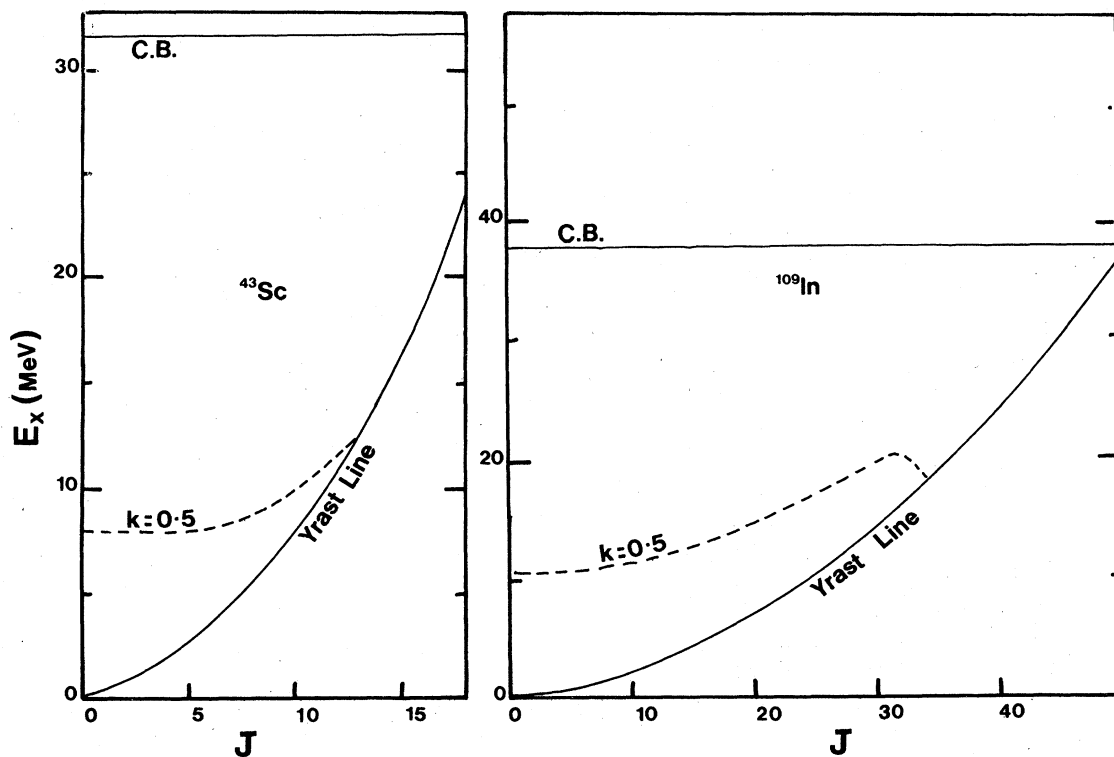
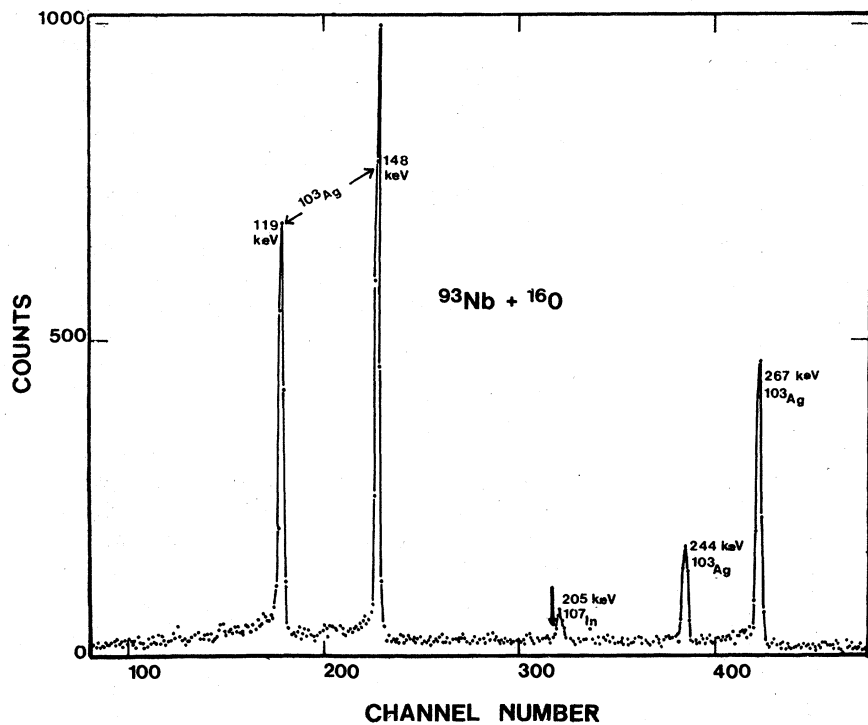
The upper limit presented here for the  $^{27}\text{Al}(^{16}\text{O}, \gamma)^{43}\text{Sc}$  cross section ( $\bar{\sigma} < 0.2 \mu\text{b}$ ) is consistent with the results of Coleman *et al.*<sup>4</sup> made at lower energies ( $\bar{\sigma} < 0.2 \mu\text{b}$ ). However, both the  $^{27}\text{Al}(^{16}\text{O}, \gamma)^{43}\text{Sc}$  and  $^{93}\text{Nb}(^{16}\text{O}, \gamma)^{109}\text{In}$  results are smaller by a factor of  $\sim 100$  than those for  $^{30}\text{Si}(^{14}\text{N}, \gamma)^{44}\text{Sc}$ ,  $^{16}\text{O}(^{32}\text{S}, \gamma)^{48}\text{Ti}$ , and  $^{40}\text{Ca}(^{12}\text{C}, \gamma)^{52}\text{Cr}$ .<sup>5, 6</sup> This finding is surprising in that the HIC processes considered by Zeller *et al.*<sup>5</sup> and Imazato<sup>6</sup> would not be expected to give rise to such large differences in the cross sections. In particular, the cross sections for the  $^{27}\text{Al}(^{16}\text{O}, \gamma)^{43}\text{Sc}$  and  $^{30}\text{Si}(^{14}\text{N}, \gamma)^{44}\text{Sc}$  would be expected to be approximately equal in magnitude since the entrance channel Coulomb-barrier heights are approximately equal, the relevant  $Q$  values are very nearly equal and the populations of compound nuclear states versus angular momentum given by optical model calculations are similar in each case. To gain more insight into these disparities, crude estimates of the cross sections for the  $^{27}\text{Al}(^{16}\text{O}, \gamma)^{43}\text{Sc}$  and  $^{93}\text{Nb}(^{16}\text{O}, \gamma)^{109}\text{In}$  HIC reactions were made.

The calculations followed along the lines of those made by Imazato.<sup>6</sup> The first step was to consider  $E_x$  vs  $J$  plots for  $^{43}\text{Sc}$  and  $^{109}\text{In}$  states as shown in Fig. 6. The yrast curves were obtained using the formula

$$E_{\text{yrast}} = \frac{\hbar^2}{2I_{\text{rig}}} J(J+1). \quad (4)$$

The parameter  $I_{\text{rig}}$  was determined from the empirical relationship

$$I_{\text{rig}} = 0.014A^{5/3} \hbar^2 \text{ MeV}^{-1}. \quad (5)$$



The regions shown in Fig. 6 which are bounded by the  $k = \Gamma_\gamma/\Gamma = 0.5$  line and the yrast line are regions of low-lying states that decay predominantly by  $\gamma$  emission to other states in the region. The  $k = 0.5$  line was obtained from calculations using the statistical model computer program GROGGI.<sup>9</sup> For these calculations,  $p$ -,  $n$ -, and  $\alpha$ -transmission coefficients were determined using optical model parameters given in Refs. 10 and 11. The  $\gamma$ -ray partial widths were fixed somewhat arbitrarily to be such that the  $E1$ ,  $M1$ , and  $E2$  transition strengths corresponded to 0.01, 0.1, and 1 Weisskopf units (W.u.), respectively, which are approximately the average values given by the compilation of Skorka *et al.*<sup>12</sup> It should be noted, however, that the position of the  $k = 0.5$  line was only weakly dependent on the  $\gamma$ -ray strengths used.

The initial population of compound nuclear states versus  $J$  was obtained from optical model calculations using optical model parameters from Ref. 10. An example of these data is shown in Fig. 7. The probabilities for populating lower states by statistical  $\gamma$  decays with energies up to  $E_\gamma = 26$  MeV were calculated using the program GROGGI.<sup>9</sup> These results were extrapolated to lower excitations under the assumption that states with  $E_x, J$  are populated according to

$$P(E_x, J) \propto \omega(E_x, J) E_\gamma^{2L+1}, \quad (6)$$

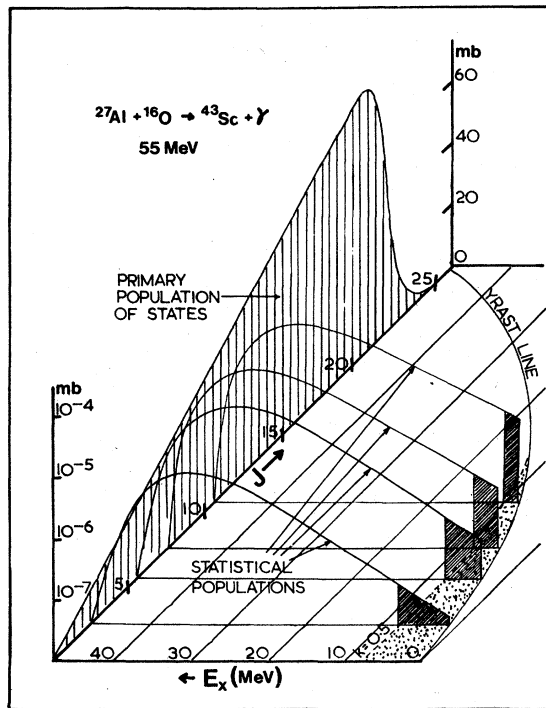


FIG. 7. Diagram illustrating HIC calculations for  $^{27}\text{Al}(^{16}\text{O}, \gamma)^{43}\text{Sc}$  reaction at 55 MeV.

where  $\omega(E_x, J)$  is the density of states and  $L$  is the multipolarity of the  $\gamma$ -ray transitions considered. Examples of these data are shown in Fig. 7. Total HIC cross sections were estimated by summing the population probabilities for all states between the  $k = 0.5$  line and the yrast line.

The calculated HIC excitation functions are shown in Fig. 8. The cross sections peak near the Coulomb-barrier heights as would be expected since compound nucleus formation becomes increasingly more inhibited as the energy is decreased below  $E_c$  and competition from particle emission becomes larger as the energy is increased. The excitation function for the  $^{93}\text{Nb}(^{16}\text{O}, \gamma)^{109}\text{In}$  reaction is more peaked than that for the  $^{27}\text{Al}(^{16}\text{O}, \gamma)^{43}\text{Sc}$  reaction due to the more rapid increase in the number of decay channels with increasing energy. The fact that the relative importance of the  $E2$  contribution to the cross section is largest for the  $^{93}\text{Nb}(^{16}\text{O}, \gamma)^{109}\text{In}$  reaction arises in the main from the Weisskopf formulas which give  $\Gamma(E2) \propto A^{4/3}$ ,  $\Gamma(E1) \propto A^{2/3}$ , and  $\Gamma(M1) \propto A^0$ .

Figure 8 shows that the calculated results are

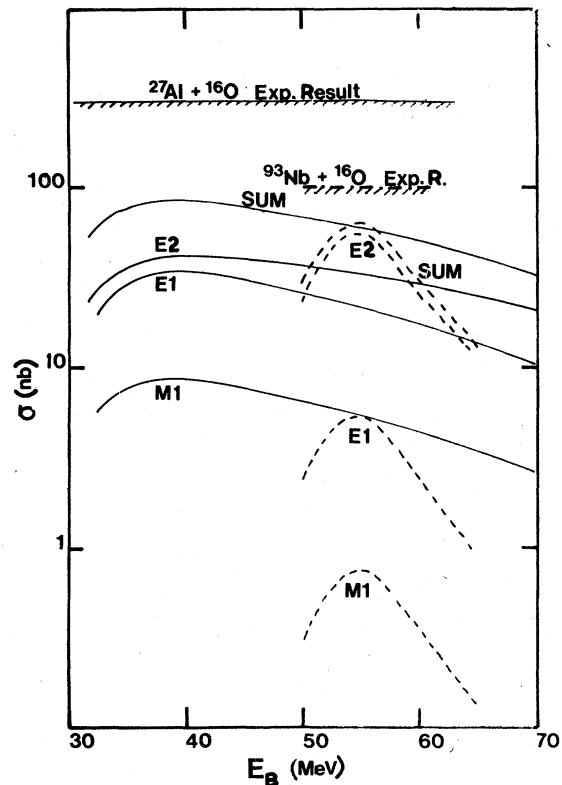


FIG. 8. Results of HIC calculations for  $^{27}\text{Al}(^{16}\text{O}, \gamma)^{43}\text{Sc}$  reaction (solid curves) and  $^{93}\text{Nb}(^{16}\text{O}, \gamma)^{109}\text{In}$  reaction (dashed curves) vs bombarding energy. The experimental upper limits presented here are also shown.

smaller than the upper limits given here and very much smaller than the results of Zeller *et al.*<sup>5</sup> and Imazato<sup>6</sup> for similar HIC studies. Although the treatment of the  $\gamma$  decays used here is crude, the statistical  $\gamma$ -decay probabilities are most probably overestimated since the averages of the  $\gamma$  data<sup>12</sup> we used are expected to be biased towards high results in consequence of the fact that weak transitions are below the level of detection. In view of this, it would appear that the previous results are probably in error.

This view is further supported in the case of the  $^{30}\text{Si}(^{14}\text{N},\gamma)^{44}\text{Sc}$  reaction by our statistical model calculations as can be seen by reference to Fig. 6. This shows that highly excited  $^{43}\text{Sc}$  states with  $E_x, J$  near the yrast line preferentially decay by particle emission; the calculation gives  $\sim 95\%$   $\alpha$  decay which is not significantly changed if the  $\gamma$  widths are increased by a factor of 1000. Assuming this situation holds for the neighboring nucleus  $^{44}\text{Sc}$ , which is highly likely in view of the consideration given earlier, then HIC by the method proposed by Zeller *et al.*<sup>5</sup> (see Sec. I) is not possible. The  $^{30}\text{Si}(^{14}\text{N},\gamma)^{44}\text{Sc}$  excitation function would, therefore, be expected to decrease with increasing bombarding energy which disagrees with the reported data.

A possible explanation of how an error may have arisen in the previous work<sup>5</sup> is that the target became contaminated with traces of phosphorous or sulphur. The presence of these  $A > 30$  contaminants would be difficult to detect since the expected reaction products with  $A > 44$  either do not have suitable lifetimes for detection or are only weak  $\gamma$  emitters.

An alternative explanation could be as follows.

The  $^{14}\text{NH}_2^-$  beam that was injected into the FN tandem was almost certainly contaminated with  $^{16}\text{O}^-$  ions since these ions are generally present in direct extraction sources and the magnetic rigidities of the two beams would agree to within  $\sim 0.08\%$ . By chance occurrence, it turns out that  $^{16}\text{O}$  ions which are stripped to the  $5^+$  state in the terminal, accelerated in the high energy tube and then undergo charge exchange to the  $6^+$  state with residual gases in the section leading to the analyzing magnet, have a magnetic rigidity of 0.9988 of that for the  $^{14}\text{N}$   $6^+$  ions. There is a slight possibility, therefore, that the  $^{14}\text{N}$  beam could have been contaminated by a small  $^{16}\text{O}$  beam which would give rise to  $^{44}\text{Sc}$  nuclei through reactions on the Si target.

In the case of the  $^{16}\text{O}(^{32}\text{S},\gamma)^{48}\text{Cr}$  experiment<sup>6</sup> large corrections were made to the data based on the assumption that an  $^{18}\text{O}$  impurity was present. This, however, was not established and the presence of another impurity (e.g.,  $F$ ) would render the analysis inappropriate. Furthermore, the subtraction procedure used could lead to errors if the contaminant was not uniformly distributed throughout the target. Similar arguments apply to the  $^{40}\text{Ca}(^{12}\text{C},\gamma)^{52}\text{Cr}$  data.

In view of all the considerations made here, it would appear that there is considerable doubt as to whether HIC has been observed as yet using activation methods. Clearly, more sensitive measurements are required.

This work was performed under the auspices of the U. S. Department of Energy under contract number EY 76-C-02-3069.

\*Permanent Address: Physics Department, The University of Edinburgh, Edinburgh, Scotland.

<sup>1</sup>W. Feldman and D. W. Heikkinen, Nucl. Phys. **A133**, 177 (1969).

<sup>2</sup>A. M. Sandorfi and A. M. Nathan, Phys. Rev. Lett. **40**, 1253 (1978).

<sup>3</sup>A. M. Sandorfi, L. R. Kilius, H. W. Kee, and A. E. Litherland, Phys. Rev. Lett. **40**, 1248 (1978).

<sup>4</sup>R. F. Coleman, D. N. Herbert, and J. L. Perkin, Proc. Phys. Soc. London **77**, 52C (1961).

<sup>5</sup>A. F. Zeller, H. S. Pendl, R. H. Davis, M. E. Williams, and C. I. Delaune, Phys. Rev. C **13**, 661 (1976).

<sup>6</sup>J. Imazato, Z. Phys. **A277**, 117 (1976).

<sup>7</sup>J. R. Grover and J. Gilat, Phys. Rev. **157**, 814 (1967).

<sup>8</sup>L. C. Northcliffe and R. F. Schilling, Nucl. Data Tables **A7**, 233 (1970).

<sup>9</sup>J. R. Grover and J. Gilat, Phys. Rev. **157**, 802 (1967).

<sup>10</sup>C. M. Perey and F. G. Perey, Nucl. Data Tables **13**, 293 (1974).

<sup>11</sup>D. Wilmore and P. E. Hodgson, Nucl. Phys. **55**, 573 (1964).

<sup>12</sup>S. J. Skorka, J. Hertel, and T. W. Retz-Schmidt, Nucl. Data Tables **A2**, 347 (1967).